Ultrasound Gray Scale Ratio for the Differential Diagnosis of Papillary Thyroid Microcarcinoma and Benign Micronodule in Patients with Hashimoto's Thyroiditis

Zhijiang Han
Hangzhou First People's Hospital
Lesi Xie
Hangzhou First People's Hospital
Peiying Wei
Hangzhou First People's Hospital
Zhikai Lei
Hangzhou First People's Hospital
Zhongxiang Ding
Hangzhou First People's Hospital
Ming Zhang (zhangming01@xjtu.edu.cn)
The First Affiliated Hospital of Xi'an Jiaotong University

Research Article

Keywords: Ultrasound gray scale ratio , papillary thyroid microcarcinoma , thyroid nodule, echogenicity , Hashimoto's thyroiditis

Posted Date: August 2nd, 2021

DOI: https://doi.org/10.21203/rs.3.rs-728316/v1

Abstract

Purpose To investigate the diagnostic value of ultrasound gray scale ratio (UGSR) for differentiating papillary thyroid microcarcinomas (PTMCs) and benign micronodules (BMNs) in patients with HT.

Methods The ultrasound images of 285 PTMCs (in 247 patients) and 173 BMNs (in 140 patients) in the HT group, as well as 461 PTMCs (in 417 patients) and 234 BMNs (in 197 patients) in the non-HT group were retrospectively analyzed. All cases were confirmed by histological examinations. The gray scale values of the nodules and surrounding thyroid tissues were measured and subsequently the UGSR was calculated. Receiver operating characteristic curve was used for determining the area under the curve (AUC), optimal UGSR threshold, sensitivity and specificity in differentiating PTMCs and BMNs in the two groups.

Results The UGSRs of PTMCs and BMNs were 0.52±0.12 and 0.85±0.24 (P<0.001) in the HT group and 0.57±0.13 and 0.87±0.20 (P<0.001) in the non-HT group, respectively. The differences in the UGSRs of PTMCs were significantly different between the two groups (P<0.001), whereas the difference in the UGSRs of BMNs was not significantly different between the two groups (P=0.416). The AUC, optimal UGSR threshold, sensitivity and specificity of UGSR for differentiating PTMCs and BMNs in the HT and non-HT groups were 0.901 and 0.890, 0.727 and 0.687, 82.05% and 77.46% and 90.67% and 91.23%, respectively.

Conclusions UGSR exhibits important diagnostic value for differentiating PTMCs from BMNs in both HT and non-HT groups, and the USGR was lower in the HT group compared with that in the non-HT group.

Introduction

The echogenicity intensities of the neck strap muscle and thyroid gland are generally used as the references for evaluating the echogenicity intensity of the thyroid nodule. According to the subjective identification through the observer's naked eye, the echogenicity intensities are classified into 4 grades as follows: extreme hypoechogenicity (lower than neck strap muscle echogenicity), hypoechogenicity (lower than thyroid gland but higher than neck strap muscle echogenicity), isoechogenicity (equal to thyroid gland echogenicity) and hyperechogenicity (higher than thyroid gland echogenicity), which could also be considered as 5 grades when anechogenicity is included. The diagnostic value of hypoechogenicity and extreme hypoechogenicity for malignant tumors have been widely acknowledged[1–3]. However, the conventional 4–5 grade method has several disadvantages. Firstly, the heterogeneity among different echogenicity intensities cannot be fully reflected. For instance, all the hypoechogenicity intensities are empowered with the same diagnostic efficiency for the differentiation of malignant and benign nodules, regardless of the difference between these intensities. However, the echogenicity intensity of each nodule is a point of continuous variable, and different points orrespond to different diagnostic efficiencies theoretically. Secondly, there is great instability in using the echogenicity intensity of the neck strap muscle as a reference, which is susceptible to various factors, such as the evenness of the strap muscle

thickness, and the percentages of muscle fibers, tendons and adipose tissues. Thirdly, subjective differences in the judgment of echogenicity intensity between observers are inevitable [4–7]. Consequently, the selection of more stable reference to quantify the echogenicity intensity of thyroid nodule has important significance in improving the differential diagnosis of malignant and benign thyroid nodules.

When selecting the reference to assess the echogenicity intensity of the thyroid nodule, the surrounding thyroid tissue has the following advantages : 1) the location is adjacent to the nodule, resulting in a more intuitive comparison of the images; and 2) the changes of the gain and dynamics of the echogenicity intensities of nodules are accompanied with the corresponding changes of thyroid tissues with the same gain levels, whereas the ratio between the echogenicity intensities is relatively stable. Since 2015, the quantitative studies on the echogenicity intensity of thyroid nodules have all taken the surrounding thyroid tissue as the reference, and the ultrasound gray scale ratio (UGSR) was used to judge the echogenicity intensity of the nodule. While only 5 articles have been published to date regarding UGSR[5–9], including our previous study[7–9]. However, none of the studies was performed in patients with HT.

The pathological bases of HT include the infiltration of lymphocytes and plasmacytes, lymphoid follicle formation with germinal centers, parenchymal atrophy of thyroid tissues and varying degree of fibrosis in the thyroid gland, resulting in the changes of echogenicity intensity of thyroid tissues [10, 11]. At present, no convincing studies have been reported on whether the echogenicity intensity of nodule in patients with HT will change. We speculated that there might be certain degrees of lymphocyte infiltration in and around the nodules, resulting in lower echogenicity intensities of the nodules. However, if the echogenicity intensities of the nodule, thyroid parenchyma and muscle simultaneously decrease or increase in patients with HT, or in case one of them decreases or increases slightly, the echogenicity intensity grading of the nodule will not change, according to the traditional 4–5 grade method. In addition, the subjective difference of echogenicity judgment between observers should not be underestimated when the patients present with HT [12]. Therefore, whether there is difference in echogenicity intensity between nodules with HT and without HT needs to be confirmed by quantification.

In the present study, UGSR was used to quantitatively analyze the echogenicity intensity of PTMCs and BMNs in the HT group, and compared with that in the non-HT group, aiming to identify the diagnostic value of UGSR for differentiating PTMCs and BMNs in patients with HT and provid potential evidence for modifying TIRADS.

Materials And Methods

Study subjects

We identified a total of 3,180 consecutive patients with thyroid nodules treated in the Affiliated Hangzhou First People's Hospital, Zhejiang University School of Medicine from January 2018 to January 2021. All the cases were confirmed by histological examinations. The following nodules were excluded from the

analysis: 1) maximal diameter >1.0 or <0.4 cm; 2) cystic-dominated nodules (the cystic component was >50%) [13, 14]; 3) calcification-dominated nodules; 4) lack of TPO-Ab and/or TG-Ab examination; and 5) unqualified image quality. Finally, 1,001 patients with 1,153 thyroid nodules who met the inclusion criteria were included in the study. Fig. 1 indicated a flow chart demonstrating the characteristics of the study participants. All the procedures described in this study were done in accordance with national ethical standards and Helsinki declaration. All collected data have been analyzed and stored according to the local legal requirements, thereby ensuring the privacy and protection of individual patient data.

Ultrasonic examination

The following five ultrasonic scanners were used in the present study: MyLab 70 XVG (Genova, Italy), Esaote MyLab Classic C (Genova, Italy), Esaote Mylab 90 (Genova, Italy), mindray (Shenzhen, China) and Hitachi (Tokyo, Japan). The 5-10 MHz broadband linear array probes were used for this study and the central frequency was 7.5 MHz. The positions and scanning areas of all the patients were the same during the scanning process. In brief, the patients were placed in the supine position with the neck dorsal stretched as possible to sufficiently expose the anterior neck region. Scanning was performed on the transverse, longitudinal and oblique section, and the nodule data were recorded as follows: number, size, shape, boundary, halo around the boundary, internal echogenicity, calcification, internal and peripheral blood flow, and bilateral neck lymph nodes.

Measurement of TPO-Ab and TG-Ab

The chemiluminescence immunoassay was used for the measurement of TPO-Ab and TG-Ab, using the Siemens ADVIA Centaur XP automatic chemiluminescence immunoanalyzer (Siemens Medical Diagnosis Ltd, USA). The reference range of the antibodies was ≤60ku/L.

Pathology examination

The tissue samples were processed into slices with an average thickness of 5 μm, which were fixed in 10% neutral formalin, stained by hematoxylin/eosin (H&E), and finally examined by light microscopy. All nodules were confirmed by senior pathologists.

Image analysis

The images were assessed by two senior imaging specialists with 19 and 18 years of work experience together. They were blinded to the pathological results independently analyzed the selected cases. The gray histogram software from the RAD info reading system (Zhejiang RAD Information Technology Co., Ltd., China) was used for the measurement. The gray scale values of the nodule and surrounding thyroid tissue were measured. The same area of the contralateral side was selected for the measurement in case

of insufficient surrounding thyroid tissues on the transverse images. The larger the ROI measured, the better the representativeness of the data for the overall echogenicity intensity of the surrounding thyroid tissue. Therefore, ROI equal to or bigger than the nodule was selected in the present study to measure the surrounding thyroid tissue, which were different from previous studies where the ROIs with equal sizes were selected (8-10). For nodules with homogeneous echoes, the largest ROI was selected (Fig. 2-3). For nodules with heterogenous echoes and dominated by a certain echo-dominated region, the ROI should be as large as possible in this region (Fig. 4-5). While for nodules with mixed echoes and no echo-dominated region could be identified, the ROI should be as large as possible. Calcifications and cystic degeneration were avoided when selecting the ROIs of the nodules (Fig. 4-5). When measuring the gray scale of the surrounding thyroid tissues, the non-nodular echo region with the highest percentage in the scanning section and relatively homogeneous background echo was selected in the HT group (Fig. 5-7), avoiding the abnormal echo regions resulting from technical factors (Fig. 6-7). The centers of ROI in the nodule and thyroid tissue were preferably located at the same gain level. All cases were measured twice and the UGSR was calculated. The average value of the two measurements was calculated as the UGSR of the nodule.

Statistical Analysis

Statistical analysis was performed using SPSS 21.0 (IBM Corporation, Armonk, NY, USA) and MedCalc 16.8 (MedCalc, Ostend, Belgium). The continuous variables were reported as mean ± standard deviation or median (interquartile range), as appropriate. Categorical data are reported as numbers (%). The comparison of the categorical variables between the two groups were performed using the Pearson's chi-squared test or the Fisher's exact test, while continuous variables were compared using the independent samples t-test or the Mann-Whitney U test. Receiver operating characteristic (ROC) curve was used to explore the efficiency of UGSR in differentiating PTMCs and BMNs in the HT and non-HT groups. The area under the curve (AUC), sensitivity and specificity of UGSR in diagnosing PTMC in the two groups were compared. A *P*-value ≤ 0.05 was considered statistically significant.

Results

Distribution of sex, age, TPO-Ab and TG-Ab

The sex, age, TPO-Ab, and TG-Ab levels of patients in the HT group and non-HT group were shown in Table 1. There was no significant difference in sex distribution between PTMCs and BMNs in both HT group (P = 0.376) and non-HT group (P = 0.239). The incidences of females with PTMC and BMN were also significantly higher in HT group than in non-HT group (both P<0.001). In the two groups, the mean age of patients with PTMC was both significantly lower than that of patients with BMN (both P<0.001). The age of patients with PTMC (P=0.082) and BMN (P=0.153) was not significantly different between HT group and non-HT group. In the HT group, there was no difference in TPO-Ab (P=0.394) and TG-Ab (P=0.073) between PTMCs and BMNs. In the non-HT group, there was no significant difference in TPB-Ab

between PTMCs and BMNs (*P*=0.108), but there was significant difference in TG-Ab between PTMCs and BMNs (*P*=0.010).

Table 1

Distribution of sex, age, TPO-Ab, TG-Ab, nodule size and UGSR

Variable	HT group		Non-HT group	
	PTMC	BMN	PTMC	BMN
Sex, N (%)				
Male	14(5.67)	12(8.57)	125 (29.98)	50 (25.38)
Female	233 (94.33)	128 (91.43)	292 (70.02)	147(74.62)
Age, years	45.60(37.00, 54.00)	52.40(47.25, 59.00)	47.20(39.00, 56.00)	53.60(47.50, 62.00)
TPO-Ab	174.55(43.35, 1300.00)	186.35(32.90, 1300.00)	28.40(28.00, 39.00)	29.50(28.00, 40.65)
TG-Ab	119.30(53.33, 249.40)	138.35(76.83, 289.48)	25.00(17.60, 33.85)	21.20(15.00, 31.33)
Nodule size, mm	6.10 (4.00, 7.00)	6.95 (5.00, 9.00)	6.16 (5.00, 7.00)	7.08 (5.00, 9.00)
UGSR	0.52±0.12	0.85±0.24	0.57±0.13	0.87±0.20

Values are expressed as number (%), mean ± standard deviation, or median (interquartile range).

HT: Hashimoto's Thyroiditis; PTMC: papillary thyroid microcarcinoma; BMN: benign micronodule; UGSR: ultrasound gray scale ratio

Distribution of nodule size

The maximum diameters of PTMCs and BMNs in the two groups were shown in Table 1. The maximum diameter of PTMCs was significantly smaller than that of BMNs in the HT group (*P*<0.001) and the non-HT group (*P*<0.001). The maximum diameter of either PTMCs (*P*=0.688) or BMNs (*P*=0.523) was not significantly different between the HT group and non-HT group.

Distribution of UGSR

The UGSRs of PTMCs and BMNs in the two groups were shown in Table 1.The UGSR of PTMCs was significantly lower than that of BMNs in the HT group (P<0.001; Fig. 4-7) and the non-HT group (P<0.001; Fig. 2-3). The UGSRs of PTMCs was significantly lower in the HT group than that in the non-HT group (P<0.001), while the UGSRs of BMNs was not significantly different between the two groups (P=0.416).

Diagnostic efficiency of UGSR for PTMCs and BMNs in the two groups

The ROC curves of UGSR for differentiating PTMCs and BMNs in the two groups were shown in Fig. 8. The AUC, optimal UGSR threshold, sensitivity and specificity were 0.890, 0.687, 77.46% and 91.23% in the HT group, and 0.901, 0.727, 82.05% and 90.67% in the non-HT group, respectively (Table 2).

Table 2

Diagnostic efficiency of UGSR in the HT and non-HT groups

	AUC	Optimal threshold	Sensitivity(%)	Specificity(%)
HT	0.890	0.687	77.46	91.23
non-HT	0.901	0.727	82.05	90.67
AUC: area under the curve				

Pathological findings

The light microscopy indicated extremely low amount or no lymphocyte infiltration inside and at the margins of PTMCs and BMNs in the non-HT group (Fig. 1-2). In contrast to these observations, PTMCs and BMNs had a small to large amount of lymphocyte infiltration inside and a large amount of lymphocyte infiltration at the margins in the HT group (Fig. 3-6).

Discussion

There was no significant difference in sex distribution between PTMCs and BMNs in both HT group (P = 0.376) and non-HT group (P = 0.239). The incidences of females with PTMC and BMN were also significantly higher in HT group than in non-HT group (both P < 0.001)HT is the most common autoimmune thyroid disease and the major cause of hypothyroidism. The incidence rate of women is 4–10 times higher than that in men [15, 16]. The disease mainly occurs in patients aged 30–60 years [11, 15–18]. TPO-Ab is positive in 90% – 95% of patients and TG-Ab is positive in 60% – 80% of patients [11, 15, 16]. In the present study, the incidence of females was significantly higher than that of males in both groups, and the incidence of females was also significantly higher in HT group than in non-HT group,

which were higher than that reported by the previous studies[15, 16, 19]. The age of the patients with PTMCs was lower than the age of patients with BMNs in both groups, which could be associated with the fact that patients with malignant nodules tended to receive surgical treatment earlier. Besides, our study indicated that the TG-Ab levels in BMNs were lower than those of PTMCs in the non-HT group. We speculated that such differences could be associated with the selection of the samples. Consistent with our previous findings [9], the average size of the PTMCs in both groups was significantly lower than that of the BMNs, which might be related to the fact that the relatively small cystic BMNs were excluded from this study for not meeting the inclusion criteria.

According to the traditional 4–5 grade method of ultrasonic echogenicity intensity, most researchers believed that the echogenicity intensity was of almost equal importance in differentiating benign and malignant thyroid nodules regardless of whether HT is present or not [16, 20–23], of which the sensitivity and specificity of hypoechogenicity for diagnosing malignant nodules were 62% – 87.2% and 42.9% – 58.5%, respectively [13, 14, 24]. The present study demonstrated that UGSR was statistically significant in differentiating PTMCs and BMNs in both HT and non-HT groups, and the AUC was highly consistent (0.890 and 0.901, respectively). The optimal UGSR threshold was 0.687 and 0.727 and the corresponding sensitivity and specificity were 77.46% and 91.23%, 82.05% and 90.67%, respectively, suggesting that the diagnostic efficacy of the UGSR was substantially higher than that of the traditional 4–5 grade method [2, 13, 14]. The UGSRs of the PTMCs in the HT group were lower than in the non-HT group, while the UGSRs of the BMNs were not significantly different between the two groups.

In 2015, Grani et al. [5] discriminated the thyroid nodules in patients receiving FNAC by the UGSR of nodule to surrounding thyroid tissue and the UGSR of nodule to neck strap muscle, demonstrating that the former had higher diagnostic power than the latter. However, in their study, the sample size of malignant nodules was small and the nodules were not classified by pathological subtype and nodule size. In addition, all the nodules were confirmed by FNAC rather than histopathology. In 2018, we performed a controlled study on the UGSR of PTMCs and micronodular goiters in a single medical center [7], and further conducted a two center study in 2021 [9]. The findings of both studies demonstrated that UGSR had important value in differentiating PTMCs and micronodular goiters, and the AUC, optimal UGSR threshold, sensitivity, and specificity were highly consistent (0.895 vs. 0.918, 0.691 vs. 0.721, 86.8% vs. 88.1% and 80.4% vs. 83.3%, respectively). In 2019, Chen et al. [6] classified the papillary carcinomas and nodular goiters based on the size of the tumors, the AUC, optimal UGSR threshold, sensitivity and specificity for diagnosing smaller-sized PTCs were 0.919, 0.692, 97.5% and 72.4%, respectively. The diagnostic performance was in agreement with our previous findings[7, 9]. Although our previous studies and the study by Chen et al. improved the study by Grani et al. [5], these studies were conducted in patients with normal thyroid glands. In the present study, the AUC in the HT group, as well as the AUC and optimal UGSR threshold in the non-HT group were highly consistent with our previous studies, while the optimal UGSR threshold in the HT group was lower than that of the non-HT group and our previous findings [7, 9]. We speculated that the following two factors led to the lower UGSR in the HT group: 1) infiltration of lymphocytes resulted in decreased echogenicity intensity of PTMCs, notably in PTMCs interspersing and growing in HT background and in those with prominent lymphocyte infiltration

surrounding the tumor; 2) when measuring the gray scale of thyroid gland with HT, the ROI contained the decreased echogenicity regions caused by abundant lymphocyte infiltration, as well as the increased echogenicity regions due to fibrosis formation. Finally, the average echogenicity intensity of the whole ROI was close to that of the normal thyroid gland. Although the UGSR of the HT group was lower than that of the non-HT group, the UGSR exhibited very high specificity and relatively high sensitivity in differentiating PTMCs and BMNs in the two groups, suggesting that UGSR was also suitable for patients with HT and was of great significance for improving the diagnostic efficiency of malignant nodules in these patients.

There were several limitations in this study. First, for nodules with heterogeneous echo, or thyroid tissue with heterogeneous echo due to HT, the selection and measurement of ROI had uncertainties. In the study, the selection and measurement of the ROI was performed twice by a senior imaging specialist with 19 years' working experience, which would greatly reduce this deviation. Second, nodular goiters, nodular HT and adenomas were included as BMNs in the present study. Although we did not include all the types of BMNs, these three types could represent the majority of BMNs [25]. Our future studies will further investigate whether UGSR is also suitable for other types of BMNs. Third, the judgment of the nature of thyroid nodules requires the combination of multiple ultrasound features, such as gray level, morphology, taller-than-wide shape, and microcalcification, while the aim of this study was to investigate the value of UGSR for the differential diagnosis of PTMCs and BMNs in patients with HT. Thus, combination of UGSR with other ultrasound signs for identifying benign and malignant thyroid nodules needs to be studied further. Finally, the present study was a single-center retrospective study, while prospective studies with multiple medical centers are required to provide additional objective evidence on the values and robustness of UGSR in the two groups.

In conclusion, UGSR has important values in the differential diagnosis of PTMCs and BMNs and the optimal UGSR threshold is lower in the HT group than in the non-HT group. Sufficient understanding of these characteristics can improve the accuracy of preoperative diagnosis and provide important evidence for clinicians in selecting individualized treatment strategies.

Declarations

Acknowledgements

Not applicable.

Funding

This study was supported by the National Natural Science Foundation of China (81871337), the Medical Science Research Program of Zhejiang Province (2020RC091, 2021RC024), the Key Laboratory of Clinical Cancer Pharmacology and Toxicology Research of Zhejiang Province (2020E10021), the Key Project of Scientific and Technological Innovation in Hangzhou (20131813A08).

Authors' Contributions

M.Z. and Z.X.D. conceived the study; Z.J.H. and L.S.X. participated in the design and coordination of the study. Z.K.L analyzed the ultrasonographs. L.S.X. and Z.J.H. performed the pathological analysis. Z.J.H. and P.Y.W. undertook the statistical analysis and drafted the article. All authors read and approved the final manuscript.

Compliance with ethical standards

Conflict of interest

The authors declare that they have no conflict of interest.

Ethics

This research project was approved by the Ethics Committee of Affiliated Hangzhou First People's Hospital, Zhejiang University School of Medicine. Due to the retrospective nature of the study and the use of anonymized patient data, written informed consent for participation was waived, in accordance with the national legislation and institutional requirements.

Publisher's note

Springer Nature remains neutral with regard to jurisdictional claims in published maps and institutional affiliations.

References

1. J.Y. Kwak, K.H. Han, J.H. Yoon, H.J. Moon, E.J. Son, S.H. Park, H.K. Jung, J.S. Choi, B.M. Kim, E.K. Kim, Thyroid imaging reporting and data system for US features of nodules: a step in establishing better stratification of cancer risk. Radiology. **260**, 892–899 (2011). https://doi.org/10.1148/radiol.11110206
2. G. Russ, S.J. Bonnema, M.F. Erdogan, C. Durante, R. Ngu, L. Leenhardt, European Thyroid Association Guidelines for Ultrasound Malignancy Risk Stratification of Thyroid Nodules in Adults: The EU-TIRADS. Eur Thyroid J. **6**, 225–237 (2017). https://doi.org/10.1159/000478927
3. J. Zhou, Y. Song, W. Zhan, X. Wei, S. Zhang, R. Zhang, Y. Gu, X. Chen, L. Shi, X. Luo, L. Yang, Q. Li, B. Bai, X. Ye, H. Zhai, H. Zhang, X. Jia, Y. Dong, J. Zhang, Z. Yang, H. Zhang, Y. Zheng, W. Xu, L. Lai, L. Yin, Superficial Organ and Vascular Ultrasound Group of the Society of Ultrasound in Medicine of Chinese Medical Association; Chinese Artificial Intelligence Alliance for Thyroid and Breast

Ultrasound. Thyroid imaging reporting and data system (TIRADS) for ultrasound features of nodules: multicentric retrospective study in China. Endocrine. **72**(1), 157–170 (2021). https://doi.org/10.1007/s12020-020-02442-x

4. H. Liu, A.L. Ma, Y.S. Zhou, D.H. Yang, J.L. Ruan, X.D. Liu, B.M. Luo, Variability in the interpretation of grey-scale ultrasound features in assessing thyroid nodules: A systematic review and meta-analysis. Eur. J. Radiol. **129**, 109050 (2020). https://doi.org/10.1016/j.ejrad.2020.109050
5. G. Grani, M. D'Alessandri, G. Carbotta, A. Nesca, M. Del Sordo, S. Alessandrini, C. Coccaro, R. Rendina, M. Bianchini, N. Prinzi, A. Fumarola, Grey-Scale Analysis Improves the Ultrasonographic Evaluation of Thyroid Nodules. Medicine. **94**, e1129 (2015). https://doi.org/10.1097/MD.0000000000001129
6. X. Chen, M. Gao, L. Hu, J. Zhu, S. Zhang, X. Wei, The diagnostic value of the ultrasound gray scale ratio for different sizes of thyroid nodules. Cancer Med. **8**, 7644–7649 (2019). https://doi.org/10.1002/cam4.2653
7. Z. Han, Z. Lei, M. Li, D. Luo, J. Ding, Differential diagnosis value of the ultrasound gray scale ratio for papillary thyroid microcarcinomas and micronodular goiters. Quant Imaging Med Surg **8**, 507–513 (2018). https://doi.org/10.21037/qims.2018. 06.04
8. Z.K. Lei, M.K. Li, D.C. Luo, Z.J. Han, The clinical significance of ultrasound grayscale ratio in differentiating markedly hypoechoic and anechoic minimal thyroid nodules. J. Cancer Res. Ther. **14**, 1567–1571 (2018). https://doi.org/10. 4103/jcrt.JCRT_1031_17
9. Z. Han, N. Feng, Y. Lu, M. Li, P. Wei, J. Yao, Q. Zhu, Z. Lei, D. Xu, A Control Study on the Value of the Ultrasound Grayscale Ratio for the Differential Diagnosis of Thyroid Micropapillary Carcinoma and Micronodular Goiter in Two Medical Centers. Front Oncol. **10**, 625238 (2021). https://doi.org/10.3389/fonc.2020. 625238
10. M. Ralli, D. Angeletti, M. Fiore, V. D'Aguanno, A. Lambiase, M. Artico, M. de Vincentiis, A. Greco, Hashimoto's thyroiditis: An update on pathogenic mechanisms, diagnostic protocols, therapeutic strategies, and potential malignant transformation. Autoimmun. Rev. **19**, 102649 (2020). https://doi.org/10.1016/j. autrev.2020.102649
11. H. Guan, N.S. de Morais, J. Stuart, S. Ahmadi, E. Marqusee, M.I. Kim, E.K. Alexander, Discordance of serological and sonographic markers for Hashimoto's thyroiditis with gold standard histopathology. Eur. J. Endocrinol. **181**, 539–544 (2019). https://doi.org/10.1530/EJE-19-0424
12. I. Kim, E.K. Kim, J.H. Yoon, K.H. Han, E.J. Son, H.J. Moon, J.Y. Kwak, Diagnostic role of conventional ultrasonography and shearwave elastography in asymptomatic patients with diffuse thyroid disease: initial experience with 57 patients. Yonsei Med J. **55**, 247–253 (2014). https://doi.org/10.3349/ymj.2014.55.1.247
13. W.J. Moon, S.L. Jung, J.H. Lee, D.G. Na, J.H. Baek, Y.H. Lee, J. Kim, H.S. Kim, J.S. Byun, D.H. Lee, Benign and malignant thyroid nodules: US differentiation–multicenter retrospective study. Radiology. **247**, 762–770 (2008). https://doi.org/10.1148/ radiol.2473070944
14. G.R. Kim, M.H. Kim, H.J. Moon, W.Y. Chung, J.Y. Kwak, E.K. Kim, Sonographic characteristics suggesting papillary thyroid carcinoma according to nodule size. Ann Surg Oncol. **20**, 906–913

(2013). https://doi.org/10.1245/s10434-012-2830-4

15. F. Ragusa, P. Fallahi, G. Elia, D. Gonnella, S.R. Paparo, C. Giusti, L.P. Churilov, S.M. Ferrari, A. Antonelli, Hashimotos' thyroiditis: Epidemiology, pathogenesis, clinic and therapy. Best Pract Res Clin Endocrinol Metab. **33**, 101367 (2019). https://doi.org/10.1016/j.beem.2019.101367
16. S.M. Durfee, C.B. Benson, D.M. Arthaud, E.K. Alexander, M.C. Frates, Sonographic appearance of thyroid cancer in patients with Hashimoto thyroiditis. J Ultrasound Med. **34**, 697–704 (2015). https://doi.org/10.7863/ultra.34.4.697
17. G. Wu, D. Zou, H. Cai, Y. Liu, Ultrasonography in the diagnosis of Hashimoto's thyroiditis. Front Biosci (Landmark Ed) **21**, 1006–1012 (2016). https://doi.org/10. 2741/ 4437
18. J.Y. Lee, H.S. Hong, C.H. Kim, Prognostic value of acoustic structure quantification in patients with Hashimoto's thyroiditis. Eur Radiol. **29**, 5971–5980 (2019). https://doi.org/10.1007/s00330-019-06174-z
19. N. Slijepcevic, V. Zivaljevic, J. Marinkovic, S. Sipetic, A. Diklic, I. Paunovic, Retrospective evaluation of the incidental finding of 403 papillary thyroid microcarcinomas in 2466 patients undergoing thyroid surgery for presumed benign thyroid disease. BMC Cancer. **15**, 330 (2015). https://doi.org/10.1186/s12885-015-1352-4
20. K. Gul, A. Dirikoc, G. Kiyak, P.E. Ersoy, N.S. Ugras, R. Ersoy, B. Cakir, The association between thyroid carcinoma and Hashimoto's thyroiditis: the ultrasonographic and histopathologic characteristics of malignant nodules. Thyroid. **20**, 873–878 (2010). https://doi.org/10.1089/thy.2009.0118
21. L. Anderson, W.D. Middleton, S.A. Teefey, C.C. Reading, J.E. Langer, T. Desser, M.M. Szabunio, S.J. Mandel, C.F. Hildebolt, J.J. Cronan, Hashimoto thyroiditis: Part 2, sonographic analysis of benign and malignant nodules in patients with diffuse Hashimoto thyroiditis. AJR Am J Roentgenol. **195**, 216–222 (2010). . org/ 10.2214/AJR.09.3680
22. D. Wang, L.Y. Du, J.W. Sun, X.J. Hou, H. Wang, J.Q. Wu, X.L. Zhou, Evaluation of thyroid nodules with coexistent Hashimoto's thyroiditis according to various ultrasound-based risk stratification systems: A retrospective research. Eur. J. Radiol. **131**, 109059 (2020). https://doi.org/10.1016/j.ejrad.2020.109059
23. H. Baser, D. Ozdemir, N. Cuhaci, C. Aydin, R. Ersoy, A. Kilicarslan, B. Cakir, Hashimoto's Thyroiditis Does Not Affect Ultrasonographical, Cytological, and Histopathological Features in Patients with Papillary Thyroid Carcinoma. Endocr Pathol. **26**, 356–364 (2015). https://doi.org/10.1007/s12022-015-9401-8
24. B. Jankovic, K.T. Le, J.M. Hershman, Clinical Review: Hashimoto's thyroiditis and papillary thyroid carcinoma: is there a correlation? J Clin Endocrinol Metab. **98**, 474–482 (2013). https://doi.org/10.1210/jc.2012-2978
25. L. Yang, H. Zhao, Y. He, X. Zhu, C. Yue, Y. Luo, B. Ma, Contrast-Enhanced Ultrasound in the Differential Diagnosis of Primary Thyroid Lymphoma and Nodular Hashimoto's Thyroiditis in a Background of Heterogeneous Parenchyma. Front Oncol. **10**, 597975 (2021). https://doi.org/10.3389/fonc.2020.597975

Figures

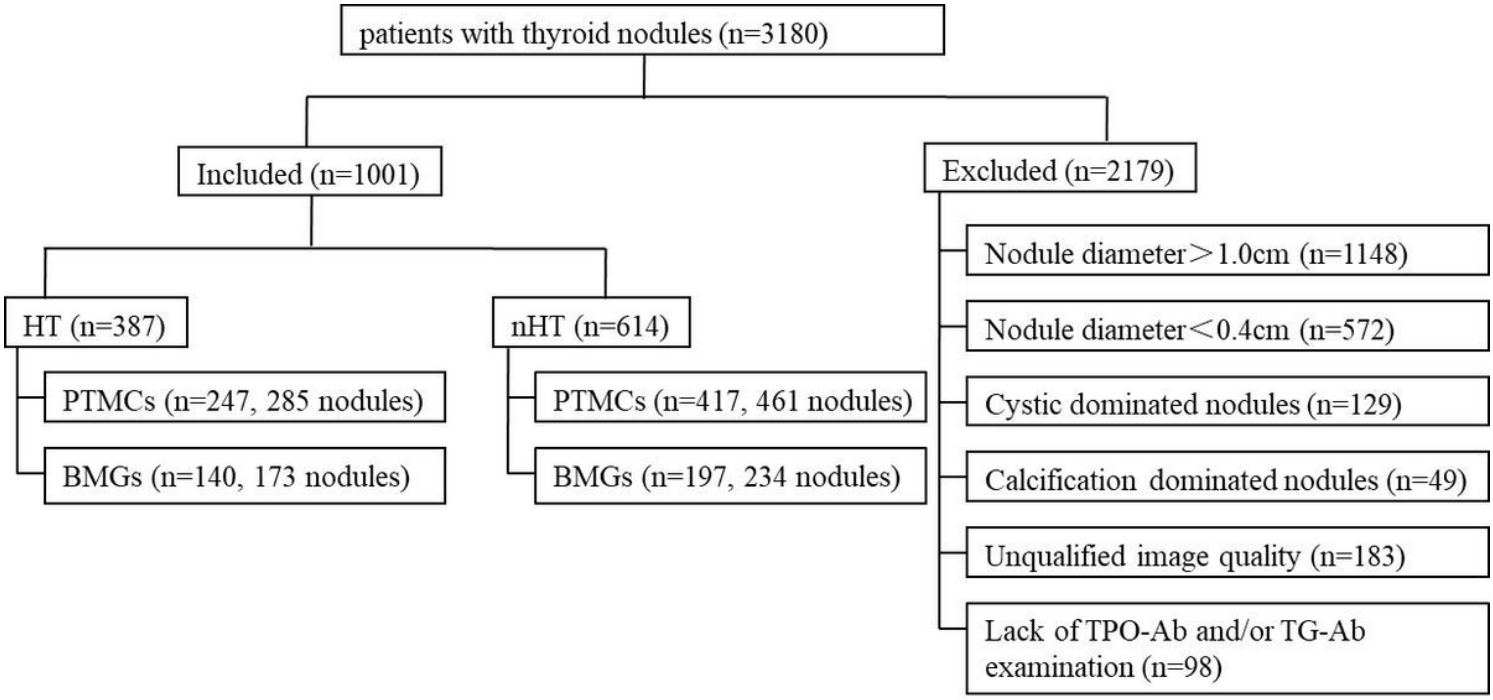

Figure 1

Flow chart of study participants.

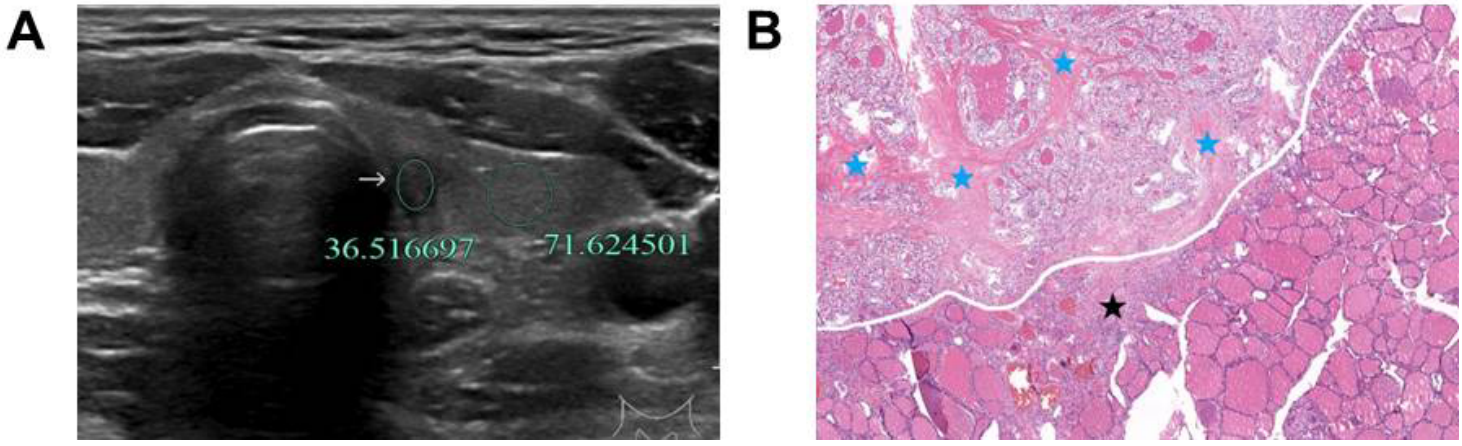

Figure 2

A 39-year-old man with PTMC in the left lobe of the thyroid. (A): the ultrasound transverse image showed that UGSR was 0.51 (36.52/71.62). (B): the pathological image (H&E × 40 magnification) displayed that the PTMC was located in the left upper part of the image, with high amounts of fiber and collagen hyperplasia (blue stars) inside the lesion, and almost no lymphocyte infiltration. The lesion and surrounding normal thyroid tissues were separated by fibers and minimal lymphocyte infiltration (black star).

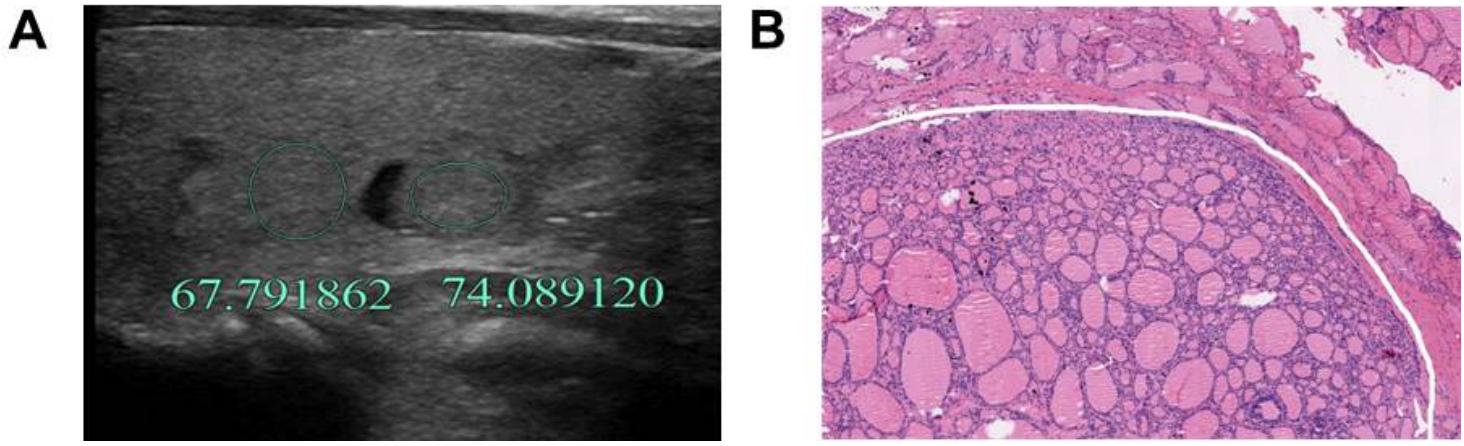

Figure 3

A 54-year-old woman with BMN in the left lobe of the thyroid. (A): the measurement was performed after avoiding the anechoic cystic region. The ultrasound longitudinal image showed that UGSR was 1.09 (74.09/67.79); (B): the pathological image (H&E × 40 magnification) indicated the presence of nodular goiter. The lesion was at the lower part of the image, which was separated from the normal thyroid tissues by fine fibers. Almost no lymphocyte infiltration was found within and around the lesion.

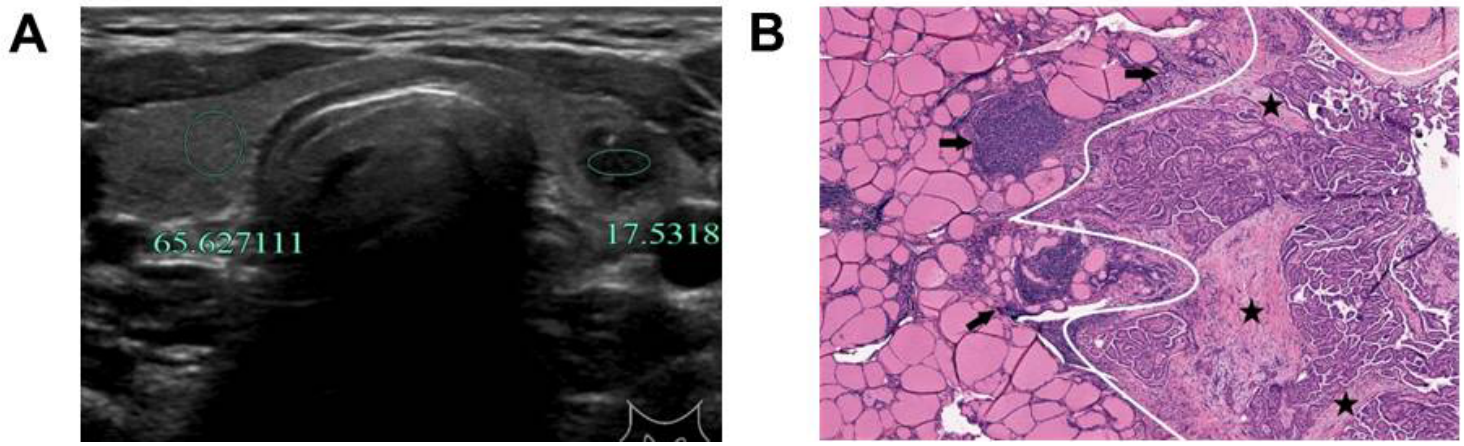

Figure 4

A 33-year-old woman with HT and PTMC in the left lobe of the thyroid. (A): calcification with hyperecho was avoided during the measurement, the ultrasound transverse image showed that UGSR was 0.27 (17.53/65.63). (B): the pathological image (H&E × 40 magnification) indicated that the presence of HT accompanied with PTMC. The right part of the image corresponded to the PTMC, in which local fiber hyperplasia and moderate amount of lymphocyte infiltration were observed (black stars), and high amount of lymphocytes infiltration (black arrows) and lymphoid follicles formation were found around the lesion.

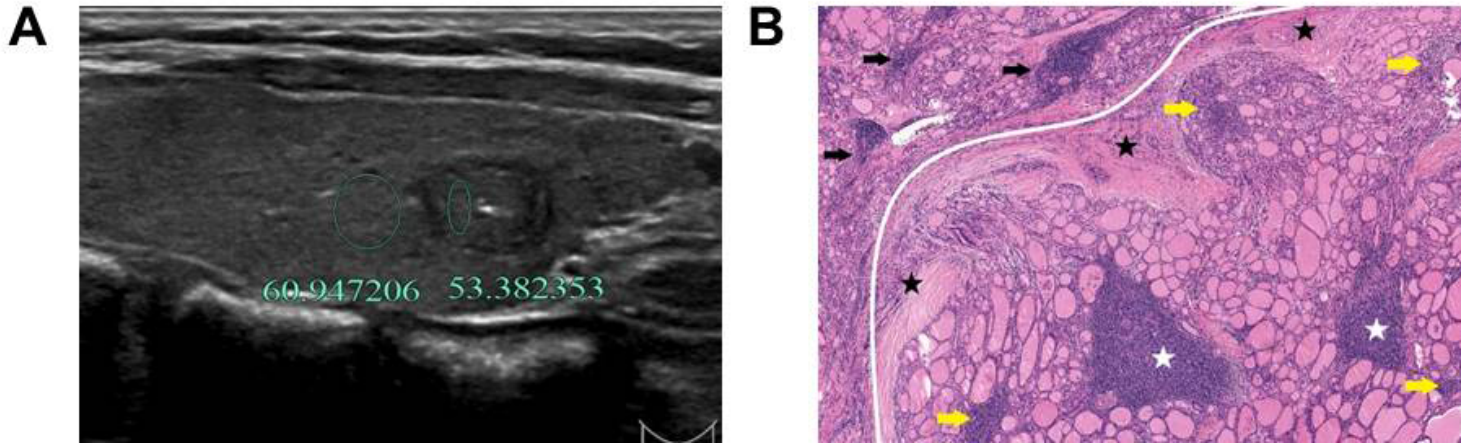

Figure 5

A 30-year-old woman with HT and BMN in the left lobe of the thyroid. (A): calcification with hyperecho was avoided during the measurement. The ultrasound longitudinal image showed that UGSR was 0.88 (53.38/60.95). (B): the pathological image (H&E × 40 magnification) demonstrated the presence of HT accompanied with nodular goiter. The right part of the image corresponded to the nodular goiter, in which high amount of lymphocyte infiltration (yellow arrows) and lymphoid follicles formation (white stars) were observed. The lesion was separated from the surrounding tissues by relatively thick fibers, which were infiltrated with moderate amount of lymphocytes (black stars). Deep infiltration of the fibers was noted in the lesion, which was surrounded with high amount of lymphocyte infiltration (black arrows).

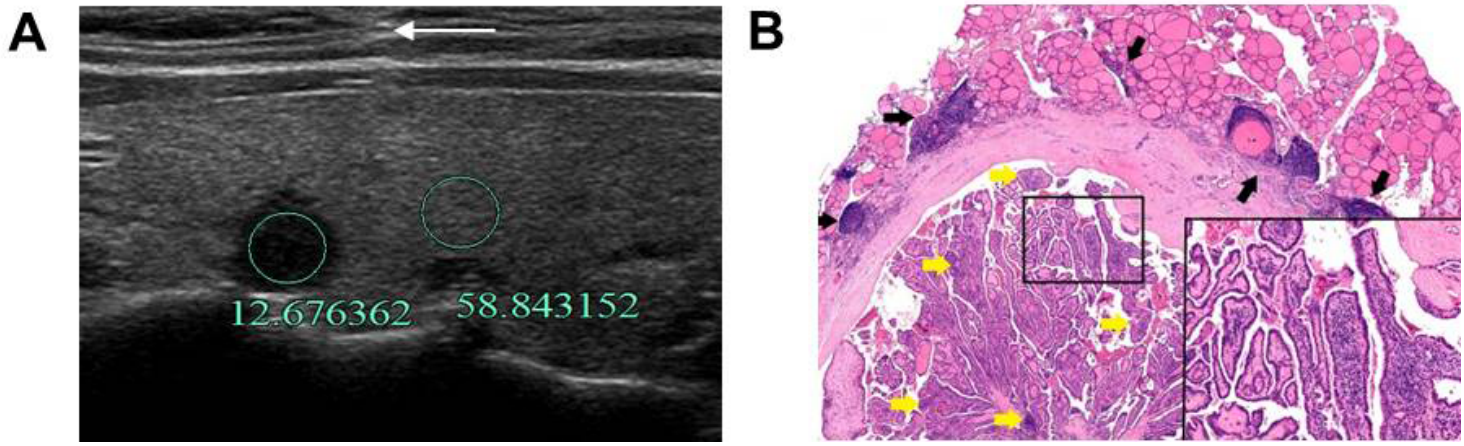

Figure 6

A 49-year-old woman with HT and PTMC in the right lobe of the thyroid. (A): the hyperecho strap resulting from technical factors was avoided (white arrow). The ultrasound longitudinal image showed that UGSR was 0.22 (12.68/58.84). (B): the pathological image (H&E × 10 magnification) indicated the presence of HT accompanied with PTMC. PTMC was localized at the lower part of the image and depicted in the black square at the right lower part of the image (H&E × 100 magnification). The lesion was separated from the surrounding thyroid tissues by thick fibers and collagens, and high amount of lymphocyte infiltration (yellow arrows) was noted in the lesion. The magnified image at the right lower part indicated

high amount lymphocyte infiltration in the central axis of the papilla and around the lesion (black arrows).

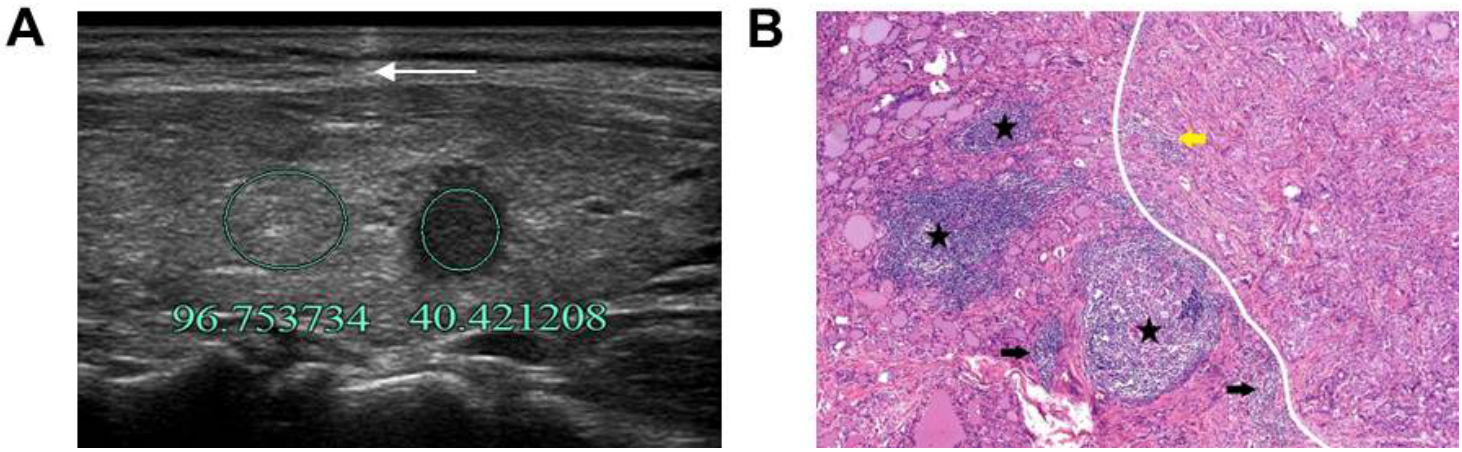

Figure 7

A 37-year-old woman with HT and PTMC in the left lobe of the thyroid. 6A. The hyperecho strap (white arrow) resulting from technical factors was avoided. The ultrasound longitudinal image showed that the UGSR was 0.42 (40.42/96.75). 6B, The pathological image (H&E × 40 magnification) indicated the presence of HT accompanied with PTMC. PTMC was at the right part of the image. Low amount of lymphocyte infiltration and fiber hyperplasia was found in the lesion (yellow arrow) and high amount lymphocyte infiltration and lymphoid follicles formation was found around the lesion (black stars).

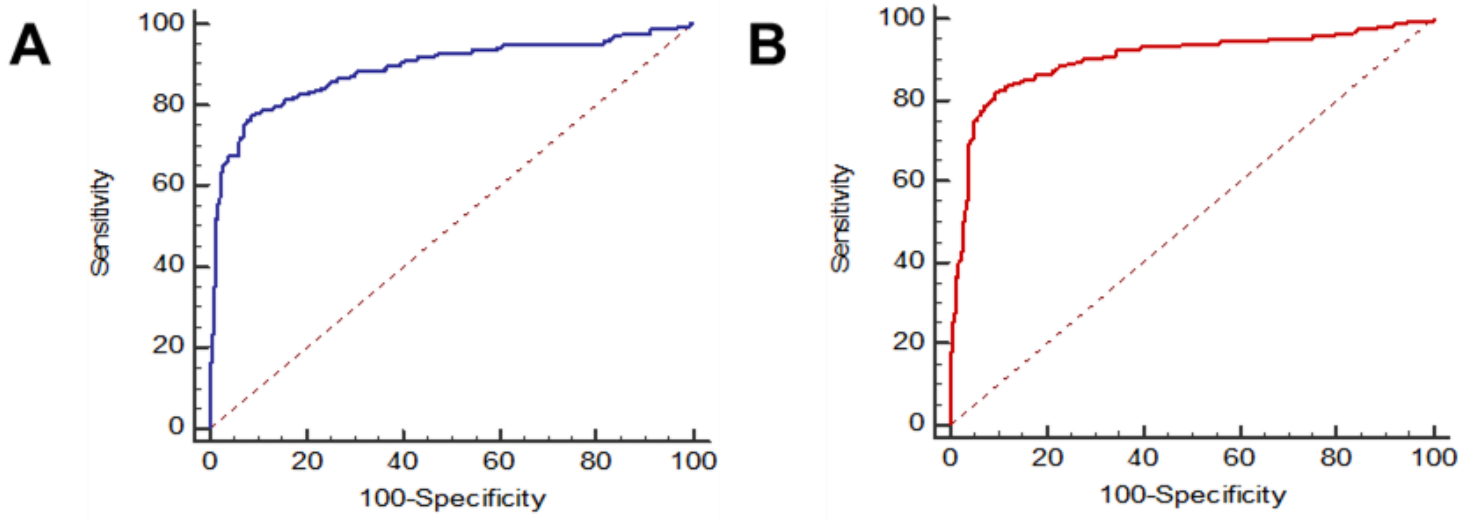

Figure 8

ROC curves of UGSR for the differential diagnosis of PTMCs and BMNs in the two groups. (A) ROC curve for the HT group. (B) ROC curve for the non-HT group.